Mitigation of the ground reflection effect in real-time locating systems based on wireless sensor networks by using artificial neural networks

Juan F. De Paz, Dante I. Tapia, Ricardo S. Alonso, Cristian I. Pinzón, Javier Bajo & Juan M. Corchado

Knowledge and Information Systems
An International Journal

ISSN 0219-1377

Knowl Inf Syst
DOI 10.1007/s10115-012-0479-8

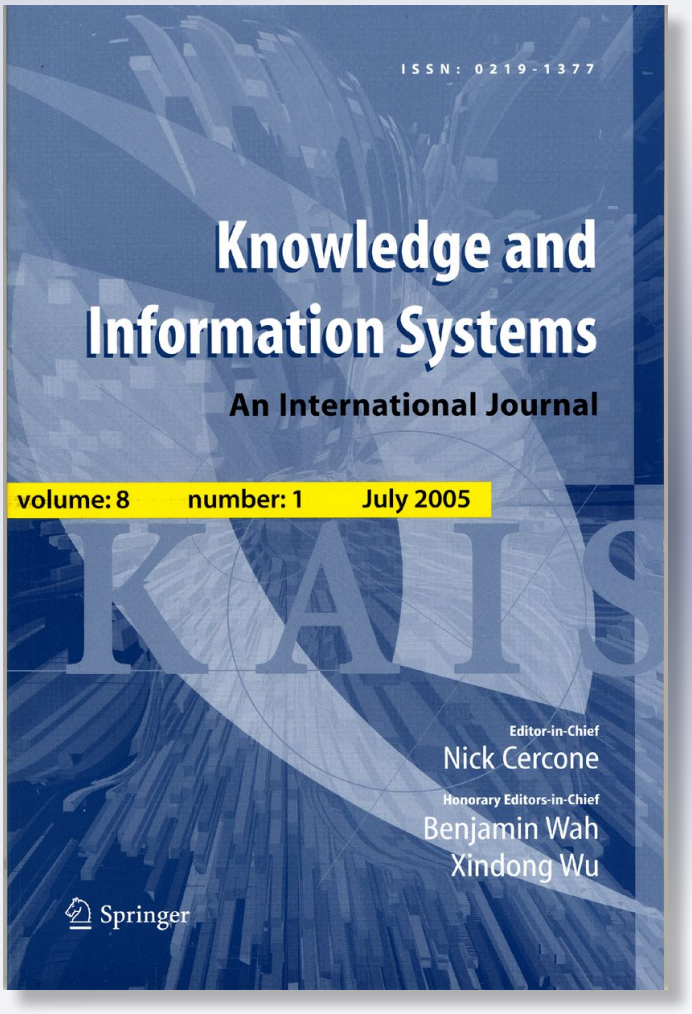

Springer

Knowl Inf Syst
DOI 10.1007/s10115-012-0479-8

REGULAR PAPER

Mitigation of the ground reflection effect in real-time locating systems based on wireless sensor networks by using artificial neural networks

Juan F. De Paz · Dante I. Tapia · Ricardo S. Alonso · Cristian I. Pinzón · Javier Bajo · Juan M. Corchado

Received: 20 April 2011 / Revised: 21 September 2011 / Accepted: 28 February 2012

Abstract Wireless sensor networks (WSNs) have become much more relevant in recent years, mainly because they can be used in a wide diversity of applications. Real-time locating systems (RTLSs) are one of the most promising applications based on WSNs and represent a currently growing market. Specifically, WSNs are an ideal alternative to develop RTLSs aimed at indoor environments where existing global navigation satellite systems, such as the global positioning system, do not work correctly due to the blockage of the satellite signals. However, accuracy in indoor RTLSs is still a problem requiring novel solutions. One of the main challenges is to deal with the problems that arise from the effects of the propagation of radiofrequency waves, such as attenuation, diffraction, reflection and scattering. These effects can lead to other undesired problems, such as multipath. When the ground is responsible for wave reflections, multipath can be modeled as the ground reflection effect. This paper presents an innovative mathematical model for improving the accuracy of RTLSs, focusing on the mitigation of the ground reflection effect by using multilayer perceptron artificial neural networks.

J. F. De Paz (✉) · D. I. Tapia · R. S. Alonso · C. I. Pinzón · J. M. Corchado
Department of Computer Science and Automation, Faculty of Computer Sciences,
University of Salamanca, Plaza de la Merced, s/n, 37008 Salamanca, Spain
e-mail: fcofds@usal.es

D. I. Tapia
e-mail: dantetapia@usal.es

R. S. Alonso
e-mail: ralorin@usal.es

C. I. Pinzón
e-mail: cristian_ivanp@usal.es

J. M. Corchado
e-mail: corchado@usal.es

J. Bajo
Faculty of Computer Sciences, Pontifical University of Salamanca,
Compañía, 5, 37002 Salamanca, Spain
e-mail: jbajope@upsa.es

Published online: 23 March 2012

Keywords Wireless sensor networks · Real-time location systems · Artificial neural networks · Ground reflection effect

1 Introduction

Wireless sensor networks (WSNs) [4] allow us to obtain information about the environment and act on this, expanding users' capabilities and automating daily actions. Some of the most interesting applications for WSNs are real-time locating systems (RTLSs). The most important factors in the locating process are the kinds of sensors used and the techniques applied to calculate the position based on the information recovered by these sensors. Although global positioning system (GPS) has provided outdoor locating services for almost two decades, and similar systems such as Galileo [27] are currently under development, indoor locating still needs much more development, especially with respect to accuracy, and low-cost and efficient infrastructures [25,33]. There is a need to develop RTLSs that perform efficient indoor locating in terms of precision and resource optimization. This resource optimization includes the reduction in the costs and size of the sensor infrastructure involved in the locating system. In this sense, the use of optimized locating techniques obtains more accurate locations using even fewer sensors and computational requirements [25].

There are several wireless technologies used by indoor RTLSs, such as RadioFrequency IDentification (RFID), wireless fidelity (Wi-Fi), ultra-wide band (UWB), Bluetooth and ZigBee [20]. However, independently of the technology used, it is necessary to establish mathematical models that determine the position of a person or object based on the signals recovered by the sensor infrastructure. The position can be calculated by means of several locating techniques, such as *signpost*, *fingerprinting*, *triangulation*, *trilateration* and *multilateration* [11,20]. However, each of these must deal with important problems when trying to develop a precise locating system that uses WSNs in its infrastructure, especially for indoor environments.

The electromagnetic waves transmitted and received by the wireless sensor infrastructure used by these systems are affected by some propagation effects, such as reflection, scattering, attenuation and diffraction [9]. Due to these effects, the energy of the transmitted electromagnetic waves is substantially modified between transmitter and receiver antennas in these systems. With the attenuation effect, it is possible to estimate the distance covered by a wave between a transmitter and a receiver antenna [2]. This is very useful for building RTLSs based on these distances or based on trilateration [20]. However, reflection, diffraction and scattering effects lead to other problems such as *multipath*, where the expected distance covered by a wave is decreased or even increased due to the sum of the waves reflected off the walls or the objects placed throughout the environment [2]. Indoor locating systems based on the measurement of distances between the sensors and the objects to be located are especially affected by the *ground reflection effect* [9], a kind of multipath propagation effect. Therefore, it is necessary to define new models and techniques that improve the accuracy of these kinds of systems. This paper proposes a new mathematical model aimed at improving the precision of RTLSs based on WSNs, especially with indoor environments. This model uses artificial neural networks (ANNs) as the main component to mitigate the ground reflection effect and calculate the position of the elements. This way, the new model proposes the use of two multilayer perceptron (MLP) ANNs [26,37] to improve the precision of RTLSs. The first MLP can mitigate the ground reflection effect when estimating distances from power signal levels used to calculate the positions of users and objects by different locating techniques. The second MLP then calculates the final positions of users and objects in the environment,

using the output of the first MLP and acting, in fact, as a new locating technique that improves the precision of other compared techniques.

This paper is structured as follows: Section 2 explains the problems that the ground reflection effect introduces in RTLSs which are based on WSNs. Related approaches that try to solve these problems partially or globally are also described. Section 3 describes a new proposal for reducing the ground reflection effect by using ANNs. Section 4 depicts a case study where the new model was applied in a real scenario, explains the experiments performed on that scenario to validate the accuracy of the new model, and describes the obtained results. Finally, Sect. 5 presents the conclusions obtained so far and depicts the related future work intended to improve the proposed method, including new applications for it.

2 Background and problem description

Real-time locating systems based on WSNs can be seriously affected by some effects related to the propagation of electromagnetic waves, especially indoors [25]. Some of these effects are *reflection*, *scattering* or *attenuation*. These effects can provoke what is known as the *multipath* effect, or the *ground reflection effect*, which is more specific to indoor RTLSs based on WSNs [14].

This section begins by depicting how RTLSs based on WSNs work, and includes some locating techniques used to estimate the position. Then, the problem of the ground reflection effect and its consequences in these kinds of systems are described, as well as some existing research that tries to solve this problem through the use of diverse approaches, including ANNs.

2.1 Real-time locating systems

The basic operation of a RTLSs begins with a network of reference nodes that are deployed throughout the area or environment where the locating will be carried out. These nodes are usually called *readers* [20]. Some of these readers can move throughout the monitored area, acting as mobile references. In addition, there is a set of mobile nodes, known as *tags* [20,33], which are carried by the users or assets to be located by the system. Each tag has a unique identifier string or number by which it is unequivocally identified in the system. Each of the tags sends a signal that contains its identifier in the system. This signal can be broadcasted periodically or as a response to other signals or excitations transmitted by the readers, also referred to as *exciters* [33]. The signals sent by the tags are detected by the readers within their coverage area. Thus, the readers can obtain the identifier of the tag that sends each signal, and also gather some measurements of that signal. These measurements provide information about the power of the received signal (e.g., RSSI or received signal strength indication), its quality (e.g., LQI or link quality indicator, its signal-to-noise ratio (SNR) or the angle of arrival (AoA) to the reader, among many others. Finally, the information (i.e., the reference measurements) from all of the readers in the network is compiled and processed in order to calculate the position of each tag. There are RTLSs in which the position is calculated by each tag (e.g., GPS); in this kind of RTLS, however, only the specific user knows its position, unless every user, or a set of them, transmits their own position to another node through a certain data communication channel, such as GPRS or UMTS [27].

Real-time locating systems can be categorized by their wireless sensor infrastructure and by the locating techniques used to calculate the position of the tags. This way, there is a combination of several *wireless technologies*, such as RFID, Wi-Fi, UWB, Bluetooth and

ZigBee, and also a wide range of *locating techniques* that can be used for determining the position of the tags. Some of the most widely used locating techniques include *signpost*, *fingerprinting*, *triangulation*, *trilateration* and *multilateration* [11,20]. The set of the locating techniques that a RTLS integrates is known as the *locating engine* [20]. Both the wireless technologies and these locating techniques will be briefly described in this and the following sections of this paper.

A widespread technology used in RTLSs is RFID [33]. In this case, the RFID readers act as exciters by continuously transmitting a radiofrequency signal that is collected by the RFID tags, which in turn respond to the readers by sending their identification numbers. In this kind of locating system, each reader covers a certain zone through its radiofrequency signal, known as *reading field*. When a tag passes through the reading field of the reader, the tag is said to be in that zone.

Locating systems based on Wi-Fi take advantage of Wi-Fi wireless local area networks (WLANs) working in the 2.4- and 5.8-GHz Industrial, Scientific and Medical (ISM) bands to calculate the positions of the mobile devices (i.e., tags) [7]. Consequently, there is a wide range of locating techniques that can be used for processing the Wi-Fi signals and determining the position of the tags, including signpost, fingerprinting or trilateration. However, locating systems based on Wi-Fi present some problems such as the interferences with existing data transmissions and the high-power consumption by the Wi-Fi tags.

Ultra-wide band (UWB) is a technology that has been recently introduced to develop these kinds of systems. As it works at high frequencies (the band covers from 3.1 to 10.6 GHz in the USA) [32], it achieves very accurate location estimations. However, at such high frequencies, the electromagnetic waves suffer great attenuation by objects (e.g., walls) so its use on indoor RTLSs presents important problems, especially the *ground reflection effect* due to the high frequencies used.

The well-known Bluetooth standard is another technology that works, as does Wi-Fi, in the 2.4-GHz ISM band and is mainly used to connect diverse devices such as mobile phones, hands free car kits or even computers, thus creating wireless personal area networks (WPANs). It can also be used to build RTLSs, mainly based on RSSI measurements and, like Wi-Fi, uses locating techniques such as signpost, fingerprinting or trilateration. Its main inconvenience is the difficulty in building WSNs made up of more than 8 devices [10].

ZigBee is another interesting technology for building RTLSs. The ZigBee standard is specifically intended to implement WSNs. As with Wi-Fi and Bluetooth, it can work in the 2.4-GHz ISM band, but it can also work in the 868- to 915-MHz band. Different locating techniques based on RSSI and LQI can be used on ZigBee WSNs (e.g., signpost or trilateration) because it can build networks of more than 65,000 nodes in star, cluster-tree and mesh topologies [20]. ZigBee is the wireless technology that was selected for our research.

As previously mentioned, RTLSs can also be categorized by the locating techniques that make up the *locating engine* (i.e., set of locating techniques). The locating engine calculates the position of each tag in the system from a set of measurements obtained from the electromagnetic waves transmitted among tags and readers. The *signpost* technique determines the area in which each tag in the environment is located according to the closest reader to each tag [20]. *Fingerprinting* is based on the previous study of some measurements of the electromagnetic waves in each zone of the monitored environment, thus making it possible to estimate in which zones each tag is located [11]. *Triangulation* calculates the position of each tag according to the angles of arrival from the broadcasted signals between tags and readers [20]. *Trilateration* calculates the position of each tag from the estimated distances between each tag and a set of readers [27]. Finally, *multilateration* estimates the position of

the tags from the time difference of arrival (TDOA) of the broadcasts received from each tag to a set of readers [8].

The measurements used by these techniques include the received power of the signals (i.e., RSSI), the quality of the received signals (i.e., LQI) or the angle of incidence to the receiver antennas (i.e., AoA). In an ideal environment, these measurements would be perfect, with no error or noise, and the calculation of tag positions would be exact. In the real world, however, the electromagnetic waves are influenced by effects such as *reflection*, *scattering*, *attenuation* and *diffraction*. Attenuation is, in fact, a desired effect for estimating distances from measurements such as the received power of signals (RSSI). RSSI can in fact be used in signpost, fingerprinting and trilateration techniques to estimate distances from signal received power. However, reflection, scattering and diffraction can make the readers receive additional spurious signals that are undesired copies of the main signal. The reception of such spurious signals makes up the multipath effect. This effect is especially undesired when measuring parameters such as the RSSI, the AoA or the TDOA. When the ground is responsible for wave reflections, multipath can be modeled as the *ground reflection effect*, which is described in the next subsection.

2.2 The ground- reflection effect

Some of the effects that influence the propagation of the electromagnetic waves include reflection, scattering, attenuation and diffraction. These effects can reduce or even increase the range of a radiotransmission [9]. The reduction or the unexpected increase in the range of a radiosignal is an important aspect to be taken into account in wireless transmission applications [2]. Specifically, these effects can be a major challenge when designing a RTLS based on WSNs, especially for indoor environments.

The detailed effects of phenomena such as attenuation and reflection in the propagation of electromagnetic waves can be calculated by solving Maxwell's equations with some boundary conditions that model the physical characteristics of each object or medium involved [9]. As this calculation can be very complex, or even the physical characteristics of each object unknown, there are few approximations to model signal propagation and calculate the range transmission. One of these approximations is the *ray-tracing* technique that simplifies electromagnetic *wavefronts* to simple particles. Physically, each *wavefront* is the locus of spatial points presenting the same phase for a certain electromagnetic wave. In the ray-tracing technique, each wavefront is considered to be a particle traveling from the transmitter to the receiver antennas. This is very useful for modeling reflection and refraction effects, although it ignores the scattering phenomenon [9].

The propagation of electromagnetic waves between antennas is a well-studied physical phenomenon. Let us consider that we have two antennas correctly aligned and polarized. Let us also suppose that these antennas are separated by a certain distance between them in free space. Finally, let us consider that the transmitter antenna is transmitting an electromagnetic wave to the receiver antenna. When transmitting a monochromatic electromagnetic wave (or a band wave narrow enough to assume a unique wavelength) through the free space between two correctly aligned and polarized antennas, the received power is given by the *Friis transmission equation* [2]:

$$P_{\mathrm{R}} = P_{\mathrm{T}} G_{\mathrm{T}} G_{\mathrm{R}} \left(\frac{\lambda}{4\pi}\right)^2 \left(\frac{1}{d}\right)^n, \tag{1}$$

where P_{R} is the power available from the receiving antenna, P_{T} is the power supplied to the transmitting antenna, G_{T} is the gain in the transmitting antenna, G_{R} is the gain in the receiving

antenna, λ is the wavelength of the electromagnetic wave in the transmission medium (e.g., the air or the vacuum), d is the distance between the transmitter and the receiver, and n is the path loss exponent that is experimentally calculated (e.g., in the free space, with no objects causing additional attenuation and reflection effects, we have that $n = 2.0$).

The wavelength of the electromagnetic wave in a medium is given by

$$\lambda = \frac{v}{f}, \tag{2}$$

where v is the phase speed of the wave in the medium ($v = c$ in the vacuum, and a lower value in any other medium) and f is the frequency of the wave.

However, this model is too ideal for real life. Applications such as RTLSs are greatly affected by the *multipath* effect, especially indoors. This means that an electromagnetic wave transmitted by a certain wireless source will be reflected, diffracted or even scattered by the multiple objects placed throughout the environment and, as a result, the antenna of the destination node will receive undesired *copies* of the transmitted signal. Even worse, these additional signals could possibly be delayed in time and shifted in frequency and phase.

When a single ground reflection effect predominates in the multipath effect, a two-ray model similar to that depicted in Fig. 1 can be used. In this model, a radiofrequency signal is transmitted through the free space from a transmitter antenna with gain G_{T} to a receiver antenna whose gain is G_{R}. The distance between the bases of the transmitter and receiver is d. The ground is assumed to be a perfect, infinite flat plain. Moreover, the height of the transmitter antenna above the ground is h_{T}, whereas the height of the receiver antenna above the ground is h_{R}. As can be seen in Fig. 1, the total energy of the signal in the receiver antenna is the sum of the energy of the wave directly transmitted between both antennas, and the energy of another wave transmitted from the transmitter antenna and reflected off the ground. This reflected wave comes in contact with the ground with an incident angle θ_i, and it is reflected with a reflection angle θ_r. In fact, by the *law of reflection*, we have that $\theta_r = \theta_i$. As the directly transmitted wave and the reflected wave travel different distances from transmitter to receiver, and the reflected wave suffers from the ground reflection, they will have a different magnitude and phase when they arrive to the receiver antenna. Due to the difference in the phases of both waves, they will be constructively or destructively added in the receiver antenna.

As both the transmission medium (typically the air) and the ground can be considered dielectric media, a portion of the incident wave on the ground is reflected by the junction

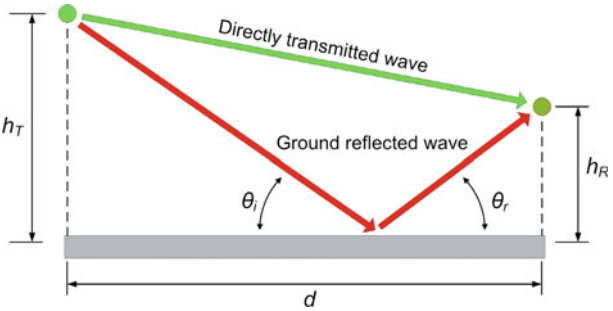

Fig. 1 Graphical representation of the ground reflection effect. Both the directly transmitted wave and the ground reflected wave travel from the transmitter antenna to the receiver antenna. They are summed up at the receiver antenna, causing the wave to be constructively or destructively added due to phase difference

between them, and the rest of the energy of the incident signal passes through this junction. This way, considering neither media to be conductive (i.e., their conductivity being $\sigma = 0$) and being that the transmission medium is the free space (relative permittivity $\varepsilon_r = 1$ and relative permeability $\mu_r = 1$), and the ground is a dielectric whose relative permittivity is ε_r and relative permeability $\mu_r = 1$, the *Fresnel reflection coefficients* for horizontal and vertical polarized signals are given by Eqs. 3 and 4, respectively.

$$\Gamma_H = \frac{\sin\theta_i - \sqrt{\varepsilon_r - \cos^2\theta_i}}{\sin\theta_i + \sqrt{\varepsilon_r - \cos^2\theta_i}}. \tag{3}$$

$$\Gamma_V = \frac{\varepsilon_r \sin\theta_i - \sqrt{\varepsilon_r - \cos^2\theta_i}}{\varepsilon_r \sin\theta_i + \sqrt{\varepsilon_r - \cos^2\theta_i}}. \tag{4}$$

For environments where $h_\mathrm{T} + h_\mathrm{R}$ is much lower than d, we have that $\Gamma_H \approx \Gamma_V \approx -1$. However, this approximation does not often suit indoor RTLSs, where distances among wireless transmitters and receivers are similar to their heights over the ground.

Figure 2 thus shows how ground reflection effect influences the transmission range between a transmitter and a receiver in the 2.4-GHz band (typical band used in Wi-Fi, Bluetooth and ZigBee) inside an office with soft partitions ($n = 2.6$, with a standard deviation $\sigma = 14.1$, and a permittivity $\varepsilon_r = 18$ for the ground), where transmitter and receiver are sited respectively at a height of 1.1 and 2.5 m above the ground. These conditions are typical for indoor RTLSs using WSNs and based on distance measurements. This figure shows how ground reflection effect varies the expected transmission range regarding the polarization of the wave. For long distances, vertical and even more horizontal polarized waves have more losses than ideally transmitted waves. Even worse, for shorter distances, the received power

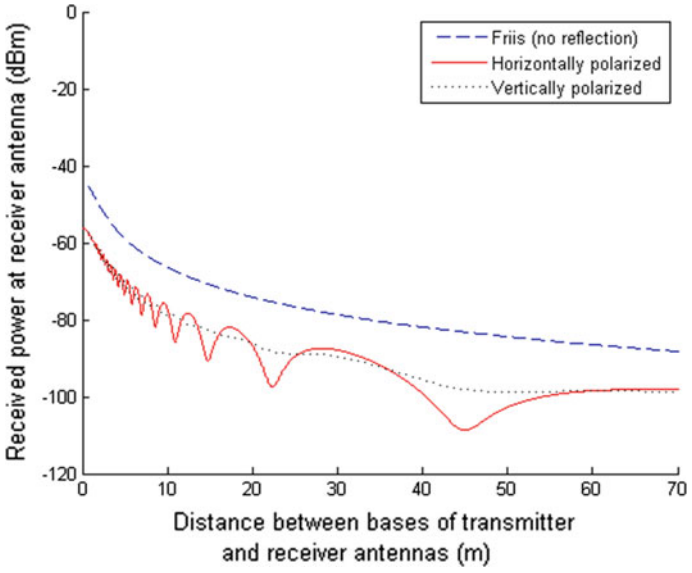

Fig. 2 Comparison of the transmission losses between the Friis free space model and the ground reflection effect model regarding the polarization of the waves. Transmitted power $P_\mathrm{T} = 0$ dBm; frequency $f = 2.450$ GHz; gain of antennas $G_\mathrm{T} = G_\mathrm{R} = 1$; height of the transmitter antenna $h_\mathrm{T} = 1.1$ m; height of the receiver antenna $h_\mathrm{R} = 2.5$ m; relative permittivity of the ground $\varepsilon_r = 18$; path loss exponent $n = 2.6$

does not vary monotonically with distance. This means that, for certain local distances, we can have a higher received power even if the receiver is sited farther away from transmitter or vice versa. Furthermore, if we want to guess the distance between a transmitter and a receiver from the received power at the receiver, we can have more than one distance between antennas that could cause such a received power.

2.3 Related approaches

There are some related approaches focused on the study or the mitigation of the multipath or the ground reflection effect. Xie et al. [35] present a multipath mitigation algorithm for a spread spectrum radiofrequency system using a frequency hopping technique and a two-ray environment. However, its integration with existing RTLS is difficult as it is based on the frequency hopping technique and requires the modification of the wireless technologies used in the systems. Eui [14] study the ranging performance through a two-ray multipath simulated model. This research uses IEEE 802.15.4a as wireless technology intended for indoor locating applications. Nevertheless, it is only a simulation with analysis proposals and does not propose a real way to mitigate the ground reflection effect. Schmitz and Wenig [30] study the wave propagation effects in the performance of Mobile Ad-Hoc WSNs and how these effects impact the routing protocol efficiency. Ray et al. [27] demonstrate how multipath effect also impacts outdoor locating systems such as GPS. This research proposes the use of a Kalman filter to estimate the errors provoked by carrier-phase multipath effect on static GPS applications. There are other approaches that use ANNs to perform locating techniques. Salcic and Chan [29] propose the use of an ANN to estimate mobile GSM phone positioning. This research includes the comparison of the ANN with a function approximation model. Nerguizian et al. [25] present a method for indoor mobile station location using received signal strength fingerprinting measurement results applied to an ANN.

The innovative mathematical model proposed in this paper takes RSSI measurements as inputs and estimates the position of the tags in the system based on these RSSI measurements. RSSI was selected because it is one of the most common measures used in current indoor RTLS and it is also easy to obtain in most wireless technologies [20]. In the first stage, the model establishes the most probable distance of each tag based on the RSSI levels by mitigating the ground reflection effect. In the second stage, the generated data are used by the model to train an MLP neuronal network [16] that finally estimates the position of each tag after the system has already been trained using standard location algorithms. This model is described in detail in the next section.

3 The new mathematical model

As previously depicted, we use the measurement of the RSSI levels of the signals sent by each tag. This way the position of each tag is estimated regardless of the position of the readers in the environment. However, two main aspects have to be taken into account when calculating the position of the tags. First of all, it is necessary to establish a relationship between the RSSI levels of the signals sent by the tags and the distances between each tag and each reader. To do this, it is necessary to model the ground reflection effect, described in Sect. 2.2, which considerably distorts the relationship between a certain range of RSSI levels and distances. It is also necessary to apply a new algorithm that can estimate the final position of each tag, based on the distances calculated according to the measured RSSI levels.

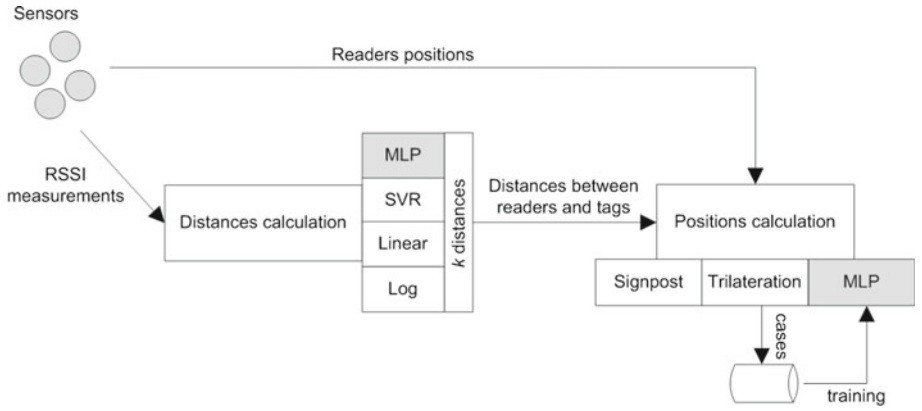

Fig. 3 Execution flows of the locating process. This *figure* shows the possible alternative executions for calculating the distances from the RSSI levels and calculating the final position of the tags from these distances

Figure 3 shows the possible execution flows for the two stages of the locating process. The first stage corresponds to the distance calculation, whereas the second stage represents the calculation of the tags' final positions. The algorithms selected for each of these stages are highlighted in gray in Fig. 3.

The next subsections analyze the ground reflection effect and the locating techniques used; each subsection describes the corresponding proposal to address these challenges.

3.1 Modeling the ground reflection effect

In ideal conditions, modeling the relationship between RSSI levels and distances between antennas creates a decaying exponential shape. This can be seen in Fig. 2 for the Friis model when ground reflection effect is not considered. Nevertheless, as shown in Fig. 2, when ground reflection effect is taken into account, the process of approximating the relationship between the RSSI levels and the distances between antennas is complex and problematic. Therefore, it is necessary to use other models that can consider the ground reflection effect in order to obtain a reliable estimate of the distances between tags and readers.

Currently, there is a wide range of models for function approximation. Among the most widely used are the *regression models*, which are based on the generation of mathematical functions that minimize a certain error function according to the training data. Usually, the error function utilized is the *least square error function*. There are different regression models for the existing relationship between the variables, including the *linear regression*, *exponential regression* or the *logarithmic regression* models, among many others. Regression models are valued according to the *coefficient of determination*, which measures the goodness of fit of a certain model.

An alternative to these regression models is the support vector regression (SVR) [6,31,34]. In SVR, it is not necessary to take into account the type of correlation between data, because the SVR method transforms the data to create linear relationships between them. The SVR method comes from a related method known as support vector machine (SVM) [15], which learns from data, and specializes in obtaining regression models by means of a change in the dimensionality of the data. SVM is a supervised learning technique that is applied to the classification and regression of different elements. It is commonly used in different fields, such as chemical [18], modeling and simulation [36], data mining [17] or text mining [21].

SVM facilitates working with data that cannot be adjusted to linear models [34] that were initially conceived to obtain classifications in linear separable problems by means of finding a hyperplane able to separate the elements of a set. In addition, SVM can also separate non-linear data. To obtain non-linear separation, SVM maps the initial data into a high dimensionality space, where the data can be linearly separated using specific functions. Given that the dimensionality of the new space can be very high, most of the time it is not viable to use hyperplanes to obtain linear separation. As a solution, non-linear functions called *kernels* are used. SVR is, indeed, a variation of SVM to generate regressions [31,34]. Therefore, the aim is to adjust the data. As in the case of SVM, the input data are mapped into a high dimensionality space in which the regression can be carried out without the initial limitations.

Polynomial interpolation methods are an alternative to regression. These methods can approximate values from a certain tabbed data set. Among the interpolation methods, we have *linear interpolation*, *Newton's divided differences interpolation polynomial*, *quadratic interpolation*, *Lagrange's interpolation polynomial*, etc. [3,19].

Other regression methods applied when the distribution of data and their relationships are unknown are *supervised learning neural networks*. These kinds of ANNs are applied in forecasting problems such as electric power consumption [12], gas consumption [26] or oil slick forecast [22]. Kalogirou [12] presents a complete review of case studies where these ANNs have been applied. Among the supervised learning networks, there are different alternatives for the learning process, which include *error-correcting learning* [28], *delta rule* or *least squares learning* [28], *generalized rule* or *error back propagation algorithm* (generalized *delta rule*) [28], *reinforcement learning* [23] or *stochastic learning* [5]. Among the supervised learning networks, we have the MLP or the radial basis function (RBF) networks [1]. ANNs are applied to a wide range of function approximation problems. Kolmogorov [13] demonstrated that given any continuous function $f : (0, 1)^n \rightarrow R^m$, $f(x) = y$, such a function can be exactly implemented by means of a three-layer feed-forward back propagation ANN with n process elements in the input layer, m elements in the output layer and $(2n + 1)$ elements in the hidden layer. Therefore, the values of the layers are obtained from

$$z_k = \sum_{j=1}^{n} \lambda^k \psi(x_j + \varepsilon \cdot k) + k \quad k = 1, \ldots, 2n + 1, \tag{5}$$

$$y_j = \sum_{k=1}^{2n+1} g_j(z_k) \quad j = 1, \ldots, m, \tag{6}$$

where z_k is the output of the k-th neuron in the intermediate layer, y_j is the output value of the j-th neuron in the output layer, λ is a real constant, ψ is a monotonically increasing real function, ε is a rational constant, and g_j is a real continuous function known as the *transfer function*.

The problem with the Kolmogorov theorem is that it mentions the existence of ψ and g_j, but it does not state how to implement these functions. The *sigmoid activation function* is thus habitually used in the intermediate layers, whereas in the output layer a sigmoid or a linear activation function can be applied. If sigmoid activation functions are chosen for the different layers, we can obtain the expressions for estimation and learning.

In the MLP, when taking into account the activation function f_j, the calculation of the output values in a hidden neuron is given by the following expression:

$$y_j^p = f_j\left(\sum_{i=1}^{N} w_{ji}(t) x_i^p(t) + \theta_j\right), \tag{7}$$

where w_{ji} represents the weight that joins j-th neuron in the hidden layer with i-th neuron in the input layer, t is the time instant, and p is the pattern in question. $x_i^p(t)$ is the i-th input value in the pattern p, N is the number of neurons in the input layers, and θ_j is the bias. The calculation of the output in a neuron in the output layer is calculated in a similar way, taking the hidden layer as an input layer.

The training for the network is carried out by the error back propagation algorithm [16]. The weights and biases for the neurons in the output layer are updated by the following expressions:

$$w_{kj}^p(t+1) = w_{kj}^p(t) + \eta\left(d_k^p - y_k^p\right)\left(1 - y_k^p\right)y_k^p y_j^p + \mu\left(w_{kj}^p(t) - w_{kj}^p(t-1)\right). \quad (8)$$

$$\theta_k^p(t+1) = \theta_k^p(t) + \eta\left(d_k^p - y_k^p\right)\left(1 - y_k^p\right)y_k^p + \mu\left(\theta_k^p(t) - \theta_k^p(t-1)\right). \quad (9)$$

The neurons at the intermediate layer are updated by a procedure similar to the previous one using the following expressions:

$$w_{ji}^p(t+1) = w_{ji}^p(t) + \eta\left(1 - y_j^p\right)y_j^p\left(\sum_{k=1}^{M}\left(d_k^p - y_k^p\right)\left(1 - y_k^p\right)y_k^p w_{kj}\right)x_i^p + \mu\left(w_{ji}^p(t) - w_{ji}^p(t-1)\right), \quad (10)$$

$$\theta_j^p(t+1) = \theta_j^p(t) + \eta\left(1 - y_j^p\right)y_j^p\left(\sum_{k=1}^{M}\left(d_k^p - y_k^p\right)\left(1 - y_k^p\right)y_k^p w_{kj}\right) + \mu\left(\theta_j^p(t) - \theta_j^p(t-1)\right), \quad (11)$$

where w_{kj} represents the weight that joins j-th neuron in the intermediate layer with k-th neuron in the output layer, t is the time instant, and p is the pattern in question. d_k^p represents the desired value, y_k^p the value obtained from k-th neuron in the output layer, y_j^p the value obtained from j-th neuron in the intermediate layer, η the learning rate and μ the momentum. θ_k^p represents the k-th bias value from the output layer. The variables for the intermediate layer are defined analogously, keeping in mind that i represents the neuron in the input layer, j is the neuron in the intermediate layer, and M is the number of neurons in the output layer.

Artificial neural networks can also work with time series. The use of time series facilitates the forecast if it is not possible to estimate non-independent values with consecutive samples. This way, a more realistic forecast of values is provided. Indeed, this is a fundamental feature for the forecast of distances from the RSSI levels, thus mitigating the ground reflection effect. This is because the ground reflection effect mainly occurs inside certain ranges of the distances.

3.1.1 Mitigation of the ground reflection effect using multiple readers

As shown in Fig. 2, the ground reflection effect registered in the signals varies according to the RSSI level. The figure demonstrates that for a certain range of RSSI values, there are fluctuations in the distance values according to the RSSI levels. Thus, a certain RSSI value can represent distinct distances. In order to model the ground reflection effect, we utilized time series applied to ANNs. Specifically, we used a MLP, as previously mentioned. ANNs can forecast a value according to the received historical values. Therefore, the neural network in this study is provided as input with both the current detected RSSI value and the RSSI values detected in previous time instants; this is how we intend to mitigate the ground

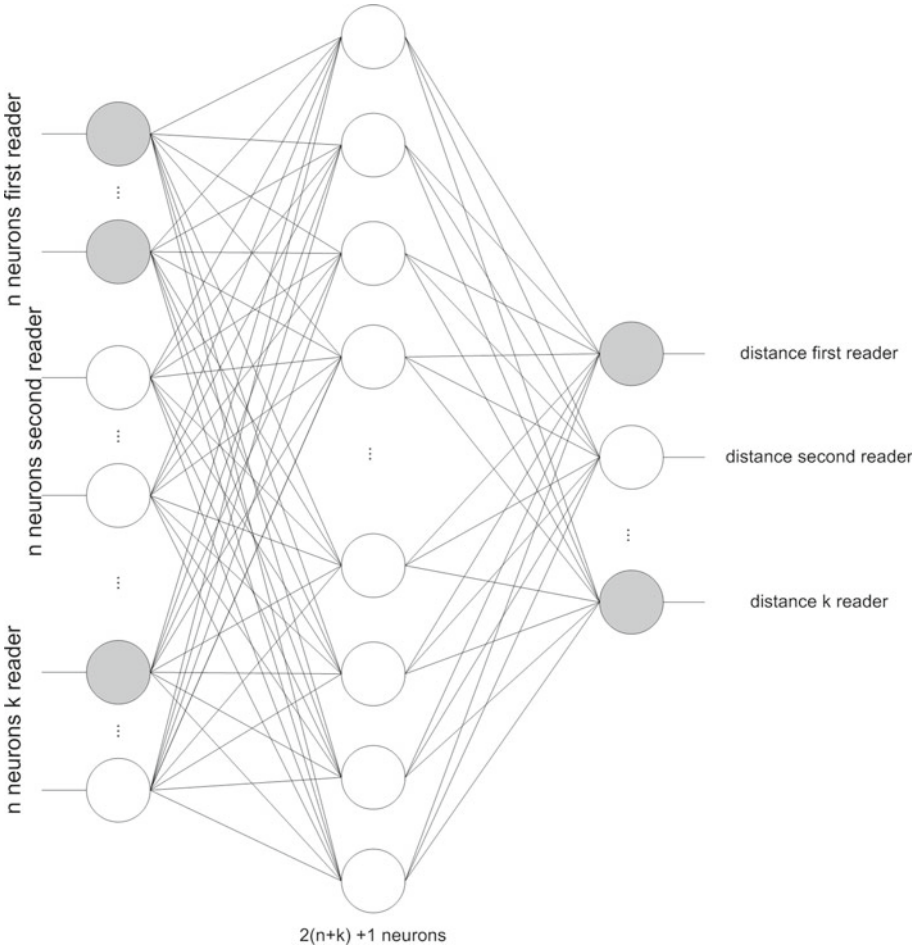

Fig. 4 Structure of the multilayer perceptron used in the training stage for the mitigation of the ground reflection effect using multiple readers. The ANN contains n inputs for each of the k readers and k outputs

reflection effect. The neural network is made up of n input neurons, being n the time instants taken into account: $t, t-1, \ldots, t-(n-1)$. The intermediate layer of the neural network is configured following the Kolmogorov theorem [13] and choosing $2n+1$ neurons.

In order to improve the forecast of the time series, we opted to incorporate the RSSI levels provided by other readers into the neural network. This way, the distance forecasting is done using a subset of the deployed readers in the system simultaneously. The architecture of the neural network is depicted in Fig. 4. This neural network has k input groups with n neurons in each of them. These n neurons correspond to the n values of the time series. Likewise, the k groups correspond to the number of readers that are considered for the distance estimation. This number of readers is set in advance; thus, the readers with the highest measured RSSI levels from the tag are selected. The intermediate layer is made up of $2(k+n)+1$ neurons, whereas the output layer is formed by k neurons (i.e., a neuron per each reader).

The groups of input neurons are ordered according to the current RSSI level from highest to lowest. Therefore, the first output of the neurons is associated with the reader that received the highest RSSI level, and so on.

3.2 Locating techniques

As previously mentioned, there are several locating techniques that can set up the *locating engine* of a RTLSs. In our research, we are focused on three of them: *signpost*, *finger printing* and *trilateration*.

The *signpost* technique is the simplest one and has a relatively low computational complexity [20]. In signpost, the location of each tag is estimated from the strongest signal received from each reader, or from the strongest signal received at each reader from each tag, according to which elements are broadcasting their identifiers. In our research, the latter estimation is used, so the tags are responsible for broadcasting their identifiers to the readers. This technique does not obtain the estimated coordinates of the position of each tag, but does obtain the zone where each tag is located. That is, it determines the closest reader to each tag in the environment. The accuracy provided by signpost can be increased by adding more readers to the wireless infrastructure (i.e., the reader density or number of readers per unit area). However, it needs more readers to achieve similar accuracy levels than other techniques.

The *fingerprinting* technique is based on the study of the characteristics of each area of locations (e.g., buildings), performing measurements of distinct radiofrequency characteristics and estimating in which area of influence each tag is found [11]. In our research, we used the RSSI levels of the signals broadcasted by the tags to the readers. However, this technique is not very dynamic, because such radiofrequency characteristics can change over time as a result of changes in the walls, the furniture or the same elements to be located. Consequently, some kind of *training* or *pre-tuning* is necessary before starting the algorithm runtime, when the actual performing of the calculation of tags' positions is done.

Trilateration, sometimes wrongly confused with *triangulation*, is a technique that calculates the position of each tag from the distance to several readers. Graphically, it is performed by an intersection of several spheres in a three-dimensional space. The distances to the reference nodes are estimated by different measurements of the received signals, such as the *Time of Flight*, the RSSI or the LQI. In our research, as in the other applied techniques, we used the RSSI levels of the signals broadcasted by the tags to the readers. This technique requires at least four reference points to determine the position of a tag in the tridimensional space. However, unlike triangulation, devices (i.e., tags and readers) do not need to use arrays of antennas on receivers, so they are simpler and cheaper than those used in triangulation-based systems [20].

Our proposed model captures data from the estimation of the positions by the trilateration algorithm. It stores these in a memory for subsequent use in carrying out the training of an MLP. This way, the neural network allows us to make the fastest estimations and is more responsive to variations in the distances resulting from the reflections of the emitted waves. Input data in the neural network correspond to the distances calculated by means of the MLP described in Sect. 3.1.1 from a pre-fixed number of readers and the position of the readers. These readers are selected according to the lowest distances they have to the tag. Output has two coordinates, one for each coordinate in the two-dimensional Cartesian space. The number of neurons in the hidden layer is $2n + 1$, where n is the number of neurons in the input layer. Finally, there is one neuron in the output layer. The activation function selected for the different layers is the *sigmoid*. Furthermore, the neurons exiting from the hidden layer of the neural network contain *sigmoidal* neurons. Network training is carried out through the *error back propagation algorithm* [16].

4 Case study

In order to test the performance of this model in an indoor environment, we proceeded to deploy a WSN infrastructure made up of several ZigBee nodes (i.e., readers and tags). As previously mentioned, the ZigBee standard is specifically intended to implement WSNs and operates in the frequency range belonging to the ISM radioband, specifically in the 868-MHz band in Europe, the 915-MHz band in the USA and the 2.4-GHz band throughout most of the world. The underlying IEEE 802.15.4 standard is designed to work with low-power and limited computational resources. The ZigBee standard allows more than 65,000 nodes to be connected in a star, tree or mesh topology. Therefore, RTLSs can implement ZigBee, allowing for the use of different locating techniques.

Each ZigBee node in our case study included an 8-bit RISC (Atmel ATmega 1281) microcontroller with 8KB of RAM, 4 KB of EEPROM and 128 KB of Flash memory and an IEEE 802.15.4/ZigBee transceiver (Atmel AT86RF230) [24]. These devices, called n-Core® Sirius A for readers and Sirius B for tags, have both 2.4-GHz and 868/915-MHz versions and have several communication ports (GPIO, ADC, I2C, PWM and USB/RS-232 UART) to connect to distinct devices, including a wide range of sensors and actuators. The n-Core® Sirius devices form a part of the n-Core platform [24], which offers a complete API (Application Programming Interface) to access all its functionalities.

The ZigBee network was formed by 15 fixed nodes acting as readers and distributed throughout three rooms, following the distribution shown in Fig. 5. The total size of the monitored area was 19 m per 19 m. The readers were distributed in this way, so that each tag could be identified by several readers simultaneously. Therefore, the selected locating techniques (i.e., *signpost*, *fingerprinting* and *trilateration*) could be applied using several simultaneous measurements.

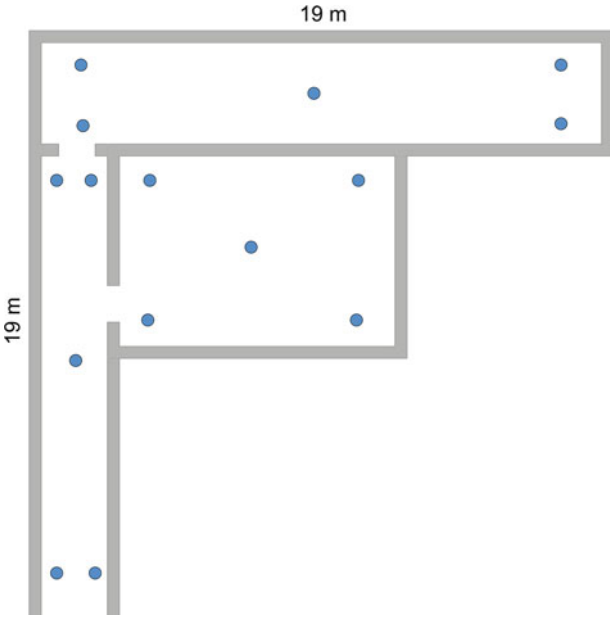

Fig. 5 Distribution of the network of ZigBee readers in the laboratory. Each *blue dot* represents a reader in the laboratory (color figure online)

4.1 Experiments

The designed neural network was compared to other regression methods and SVR in order to evaluate the results of the estimation of the distances from RSSI levels. Function interpolation methods were discarded because RSSI levels are discrete values in the ZigBee devices used in this case study (and in most wireless technologies), so it is not useful to apply these kinds of methods. The regression methods were chosen according to the representation of the information. As can be seen in Fig. 6, the logarithmic regression model fits the distribution of data.

Prior to estimating the position of the tags, we carried out a training process of the neural network built in order to estimate the distances between nodes from the RSSI levels. A test tag was successively moved through different predefined location sequences (i.e., zones inside the laboratory). This allowed us to calculate the relationship of the measured RSSI levels with the real distances between the tag and the readers. To do so, the detected RSSI levels between the tag and each of the 15 readers were measured. The RSSI–distances measurements were then used to make predictions in the time series. In total, 200 cases were generated to train the neural network according to the structure previously shown in Fig. 4. In addition, different positions were randomly chosen throughout the zones to generate 100 new cases and estimate each position by means of both the neural network and other approximation methods to compare them. Other methods were *SVR*, a *linear regression model* and a *logarithmic regression model*. Figure 7 shows the test positions used for calculating the relationship between the RSSI levels and the distances in the training data set. The calculation of these relationships is necessary because the characteristics of the existing materials considerably affect the detected distances.

Proper training and a cross-validation were both carried out to train the neural network. The neural network followed the architecture described in the Sect. 3.2, being the number of groups $k = 4$. The number of elements had to be greater than 3, so that the trilateration algorithm could work properly (i.e., three references are needed in a two-dimensional trilateration algorithm). The final number of elements was selected as 4 in order to reduce the error

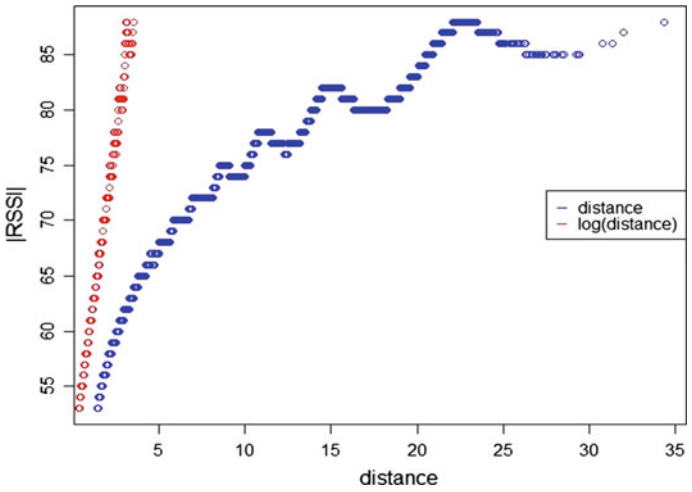

Fig. 6 Relationship between the distance and the absolute value of the measured RSSI for the ZigBee devices used in the case study

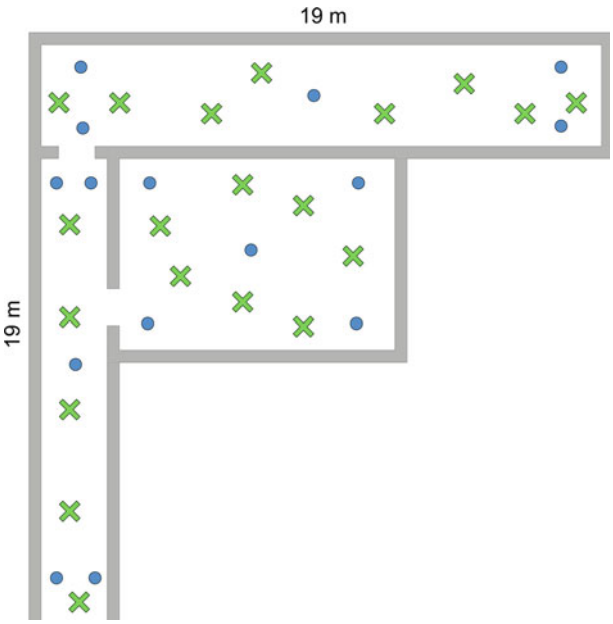

Fig. 7 Distribution of the test positions (*marked as crosses*) utilized to calculate the RSSI–distance relationships during the training of the neural network and the regression models for the mitigation of the ground reflection effect

without increasing the execution time. The number of measurements for each group was 15. This way, the number of inputs was 60. Likewise, the number of outputs was 4, one per each group. In order to generate the distinct compared models (SVR, linear and logarithmic), only the information of the group with the highest RSSI levels was used. Thus, only 15 input values and 1 output value were used in these models. Both the neural network and the other models used 200 cases of the training stage and 100 cases to make predictions.

Once the distances were calculated, the efficiency of the locating system was evaluated. This evaluation was performed by training a second neural network. The training data were obtained from the 200 initially calculated values, together with another 300 values estimated using the trilateration algorithm. The structure of the neural network is described in Sect. 3.2. The obtained results are detailed in the Sect. 4.2.

4.2 Results

Figure 8 shows the absolute errors obtained for the SVR, the linear regression model, the logarithmic model and the neural network. As can be seen in this figure, the neural network obtained better results than the other methods because it presents a lower error for the estimation of distances.

The regression model obtained for the logarithmic regression fits in a very high grade the training data, as this model obtains a $R^2 = 0.9907$. Likewise, the linear regression model obtains a $R^2 = 0.8968$, which is also a high value. Based on these R^2 values, both models can be considered as valid for estimating. That is, the estimates made are significant and any other method that improves these results would also be valid.

Figure 9 shows the relationship between the obtained error with regard to the estimator and the RSSI levels for the values used in the estimation. As can be seen in the four bar diagrams,

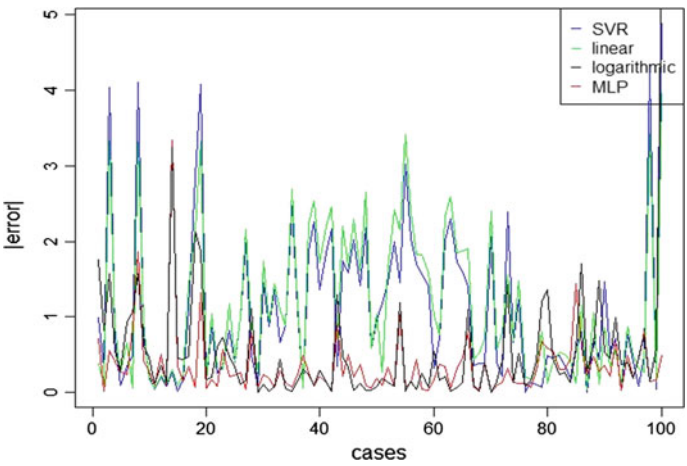

Fig. 8 Errors in estimating the distances from the RSSI levels for the different models compared: SVR, linear regression model, logarithmic model and the MLP

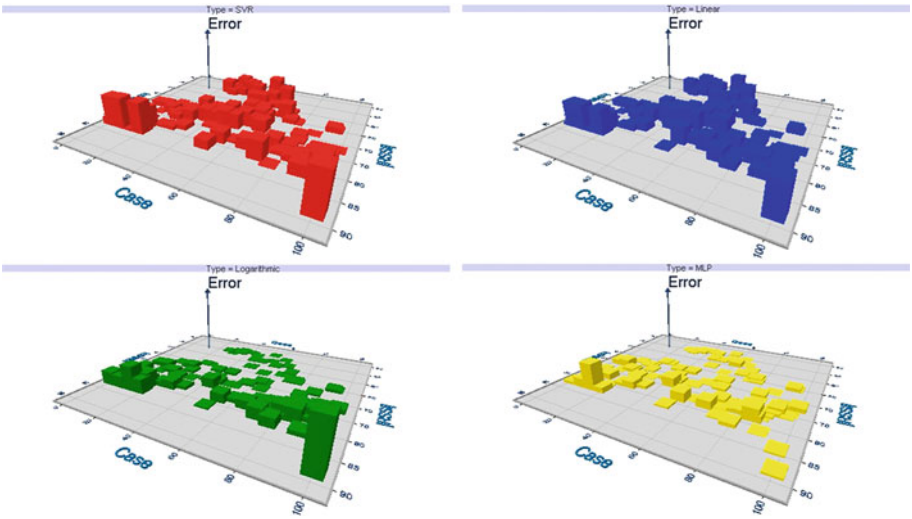

Fig. 9 Errors in the estimates of the predictions made by the different methods compared: SVR, linear regression, logarithmic regression and MLP

the errors are lower for the MLP than for the rest of the compared methods. Moreover, the errors for the MLP are concentrated in a certain range of RSSI levels. This makes it possible to create reliable values outside some specific frequency ranges.

Figure 10 shows a surface map corresponding to the highest detected errors. As can be seen, the errors obtained with the MLP are lower than those obtained with the SVR and the regression models, as almost all the detected surface is red, green or blue (the colors corresponding to SVR, logarithmic regression and linear regression, respectively).

The estimate of mean error and standard deviation for each of the models compared is shown in Table 1. As can be seen, the typical error and the deviation of the neural network are lower than those of the SVR and regression models.

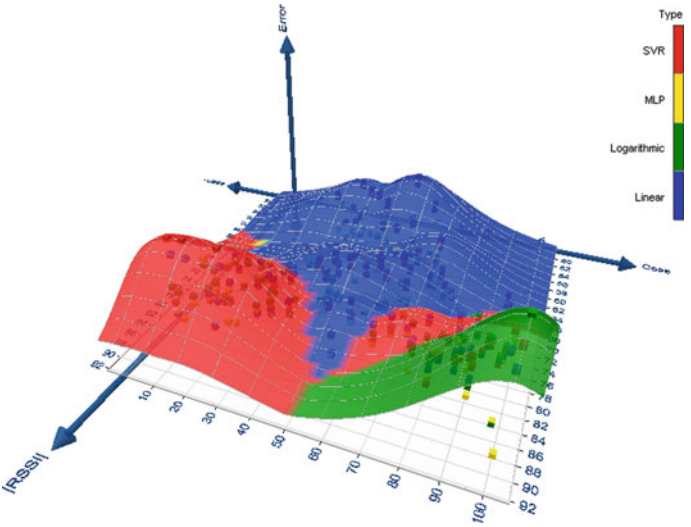

Fig. 10 *Surface map* corresponding to the highest detected errors for each of the models compared. Both the *surface* and *colors* are calculated according to the maximum error values and the kind of the error (color figure online)

Table 1 Mean error and standard deviation of the distance estimates for each of the models compared

Model	Mean	Deviation
SVR	1.09	1.04
Linear	1.16	0.98
Logarithmic	0.55	0.78
MLP	0.36	0.43

Analyzing the dispersion of the error for each of the models compared in Fig. 11, we can see that the MLP offers the lowest dispersion and does not present such extreme values as the SVR and linear regression models do. Figure 11 shows the box plot diagrams for the SVR, the regression models and the MLP. As can be seen, the MLP presents the lowest data variance.

In order to analyze the significance of the differences and to determine whether the neural network is statistically better than both the SVR and the regression models, we applied the

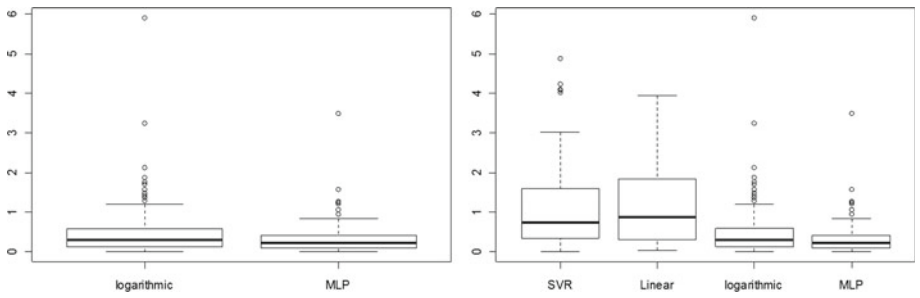

Fig. 11 Comparison of the error dispersion in the different models compared. The *figure* shows *box plots* representing the absolute error for the RSSI–distances relationship when using the different approximations

Mann–Whitney U test. This test determines two values: H_0 and H_1. H_0 shows whether the data in both groups present the same distribution, whereas H_1 determines whether there is a difference in the distribution of the error distance data. Table 2 shows the p-value obtained for the comparison method of the row and the corresponding column. Considering a significance $\alpha = 0.05$, we have that the p-value corresponding to linear–SVR and logarithmic–MLP is greater than α. Therefore, we cannot discard H_0, although it can be discarded for the equality comparisons of distributions of SVR–MLP and linear–MLP. Nevertheless, even though H_0 cannot be discarded for the logarithmic–MLP case and a significance $\alpha = 0.05$, the value that it presents, 0.1731, is low. This way, using a significance value $\alpha = 0.2$, H_0 would be discarded. Observing the information presented in Table 2, we can state that the MLP improves the results obtained by the logarithmic model.

In order to determine the position of each tag, the final positions were forecasted by applying *signpost* and *trilateration* to obtain the RSSI levels. To train the neural network, 200 positions initially realized were used, and 300 were carried out with *trilateration*. The 100 remaining measurements were used to make predictions. Figure 12 shows the absolute error obtained for the calculation of 100 positions by comparing the different methods. As can be seen, the forecast based on the neural network improves the results of the other methods and reduces the error in the predictions.

Furthermore, this improvement in the distances error is significant. To compare the different methods, the same procedure as that indicated in Table 2 was followed. The box plots representing the error information are presented in Fig. 13. As can be seen in the figure,

Table 2 Mann–Whitney's data distribution equality test for the distance errors

	SVR	Linear	Logarithmic	MLP
SVR				
Linear	0.405			
Logarithmic	3.423e-6	8.455e-8		
MLP	4.263e-10	9.696e-12	0.173	

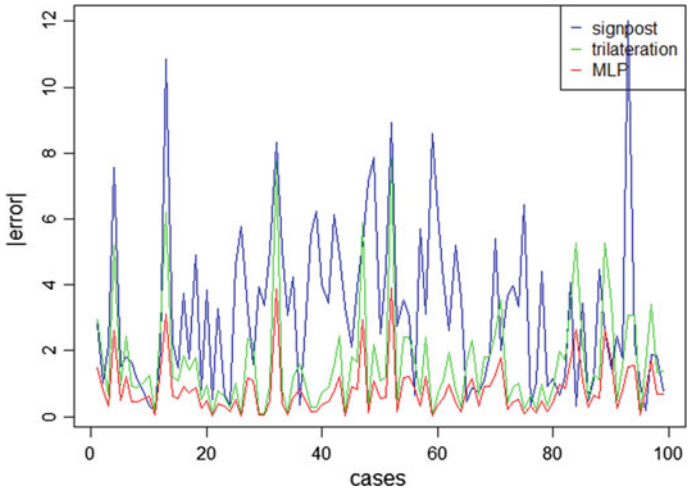

Fig. 12 Comparison of mean absolute prediction error for 100 values using signpost, trilateration and MLP

the MLP provides lower estimation errors than the signpost and trilateration by themselves, that is, without modeling the RSSI and position behaviors.

In order to compare the results obtained without using the MLP to model the ground reflection effect, the final positions were calculated by means of the logarithmic regression model. This method was chosen because it provided the best results of all the methods compared (only MLP achieved better results). Figure 14 shows the obtained results. Comparing this figure with Fig. 12, we can see that if the neural network that models the ground reflection effect is not used, the error increases in the cases of MLP and trilateration, whereas it remains constant in the case of signpost. This is because the signpost technique uses the RSSI levels directly to determine which reader is closest to each tag.

Table 3 shows the mean and the standard deviation of error obtained when the MLP or the logarithmic regression model is applied to approximate the distances from RSSI levels. As can be seen in this table, both the mean and the standard deviation of error are lower when the

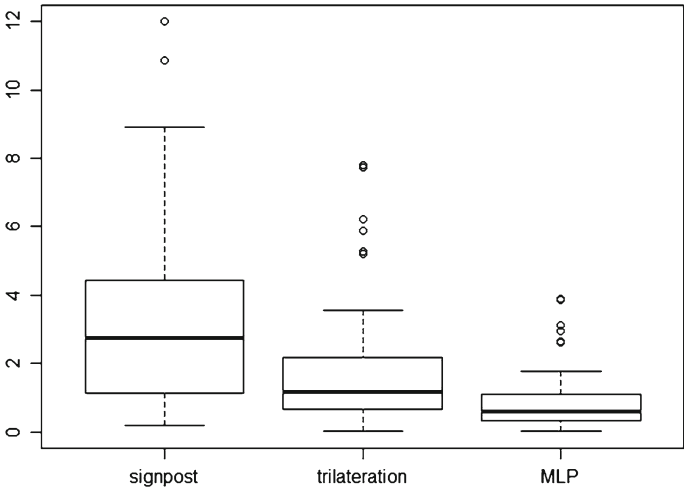

Fig. 13 *Box plot* diagrams representing the location errors for the different locating techniques compared

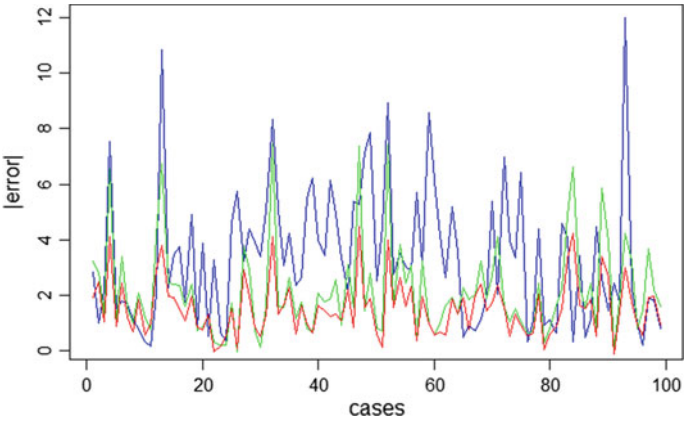

Fig. 14 Absolute error for each of the locating techniques after applying the logarithmic regression model to approximate distances

Table 3 Mean error, standard deviation (in meters) and *T* Test of the compared locating techniques after applying MLP and logarithmic regression models

Model	MLP			Logarithmic		
	Mean	Deviation	T-Test (MLP)	Mean	Deviation	*T* Test (MLP)
Signpost	3.19	2.43	2.2e-16	3.35	2.42	4.732e-9
Trilateration	1.64	1.57	3.47e-6	2.17	1.68	0.01018
MLP	0.82	0.78		1.54	1.00	

Table 4 Mann–Whitney's data distribution equality test for the distance errors using trilateration and MLP after applying the logarithmic regression model and the MLP

	Trilateration logarithmic	MLP logarithmic
Trilateration	0.003396	
MLP		
MLP		8.171e-10
MLP		

MLP was applied than when the logarithmic regression model was used. The *T* test for both approximations (MLP and logarithmic regression) was performed to determine whether the difference between MLP and the other techniques (signpost and trilateration) is significant. As can be seen in the results in Table 3, the difference between results is significant.

The result of applying the Mann–Whitney *U* test for the obtained errors is shown in Table 4. As can be seen, the differences in the calculation of the final positions when applying the logarithmic regression model or the MLP are significant. The signpost technique was not considered because it does not use distances for the calculation of the tags positions.

5 Conclusions and future work

Among the wide range of WSNs applications, RTLSs are emerging as one of the most exciting research areas available. Healthcare, surveillance or work safety applications are only some examples of the possible environments where RTLSs can be exploited. There are also different wireless technologies that can be used on these systems. The ZigBee standard offers more interesting features than the other technologies; it can use large mesh networks of low-power devices and can integrate with many other applications as it is an international standard using unlicensed frequency bands.

The operation of RTLSs can be affected by undesired phenomena such as the multipath effect, and more specifically, the *ground reflection effect*. This paper proposes a new mathematical model aimed at improving the precision of RTLSs based on WSNs. As demonstrated in this study, the use of ANNs to forecast distances from RSSI levels improves the estimation of distances when using SVR or regression models. In addition, focusing the forecast according to time series can reduce the ground reflection effect that occurs when considering only the last RSSI measurement.

The use of measurements from several readers as inputs of the MLP in the proposed model also reduces the prediction error by mitigating the ground reflection effect and improving the approximations provided by other methods with high adjustment goodness, such as the *logarithmic regression model*. This improvement in distance forecasting is very relevant when

estimating the positions of the tags, thus optimizing the overall calculations of locating techniques. The results presented in this paper demonstrate that the use of ANNs improved the approximations provided by the locating techniques. Nevertheless, a previous data gathering stage is required. In this paper, this stage was carried out both manually and automatically by means of the *trilateration* technique.

Plans for future work involve the reduction of the readers needed to perform the locating process, as well as the implementation in larger environments. Future work also includes the study of more detailed multipath models such as *Ricean* and *Rayleigh fading* or *shadowing* [30].

Acknowledgments This work has been supported by Spanish Ministry of Science and Innovation Project Ref. TRA2009_0096.

References

1. Anand P, Siva Prasad BV, Venkateswarlu Ch (2009) Modeling and optimization of a pharmaceutical formulation system using radial basis function network. Int J Neural Syst 19(2):127–136
2. Barclay LW, Engineers IOE (2003) Propagation of radiowaves. IET, London
3. Carnicer JM, García-Esnaola M (2002) Lagrange interpolation on conics and cubics. Comput Aided Geom Des 19:313–326
4. Chong SK, Gaber MM, Krishnaswamy S, Loke SW (2011) Energy conservation in wireless sensor networks: a rule-based approach. Knowl Inf Syst 28(3):579–614
5. De Gloria A, Faraboschi P, Olivieri M (1993) Clustered Boltzmann Machines: Massively parallel architectures for constrained optimization problems. Parallel Comput 19(2):163–175
6. De Paz JF, Bajo J, González A, Rodríguez S, Corchado JM (2010) Combining case-based reasoning systems and support vector regression to evaluate the atmosphere–ocean interaction. Knowl Inf Syst. doi:10.1007/s10115-010-0368-y
7. Ding B, Chen L, Chen D, Yuan H (2008) Application of RTLS in warehouse management based on RFID and Wi-Fi. Wireless communications networking and mobile computing, 2008. WiCOM '08. 4th international conference on 2008, pp 1–5
8. Galati G, Gasbarra M, Magarò P, De Marco P, Menè L, Pici M (2006) New approaches to multilateration processing: analysis and field evaluation. Radar conference, 2006. EuRAD 2006. 3rd European, pp 116–119
9. Goldsmith A (2005) Wireless communications. Cambridge University Press, Cambridge
10. Ilyas M, Dorf RC (eds) (2003) The handbook of ad hoc wireless networks. CRC Press Inc., Boca Raton
11. Kaemarungsi K, Krishnamurthy P (2004) Modeling of indoor positioning systems based on location fingerprinting. INFOCOM 2004. Twenty-third annual joint conference of the IEEE computer and communications societies. pp 1012–1022
12. Kalogirou SA (1999) Applications of artificial neural networks in energy systems: a review. Energy Convers Manag 40(10):1073–1087
13. Katsuura H, Sprecher D (1994) Computational aspects of Kolmogorov's superposition theorem. Neural Netw 7(3):455–461
14. Kim ES, Kim JI, Kang IK, Park CG, Lee JG (2008) Simulation results of ranging performance in two-ray multipath model. Control, automation and systems, 2008. ICCAS 2008. International conference on 2008, pp 734–737
15. Köknar-Tezel S, Latecki LJ (2011) Improving SVM classification on imbalanced time series data sets with ghost points. Knowl Inf Syst 28(1):1–23
16. Lecun Y, Bottou L, Orr GB and Müller KR (1998) Efficient BackProp. Lecture notes in computer science, Springer, Heidelberg, pp 5–50
17. Lessmann S, Voß S (2009) A reference model for customer-centric data mining with support vector machines. Eur J Oper Res 199(2):520–530
18. Li H, Liang Y, Xu Q (2009) Support vector machines and its applications in chemistry. Chemom Intell Lab Syst 95(2):188–198
19. Liang X-Z, Wang R-H, Cui L-H, Zhang J-L, Zhang M (2006) Some researches on trivariate Lagrange interpolation. J Comput Appl Math 195(1–2):192–205

20. Liu H, Darabi H, Banerjee P, Liu J (2007) Survey of wireless indoor positioning techniques and systems. IEEE Trans Syst Man Cybern Part C Appl Rev 37(6):1067–1080
21. Lo S (2008) Web service quality control based on text mining using support vector machine. Expert Syst Appl 34(1):603–610
22. Mata A, Corchado JM (2009) Forecasting the probability of finding oil slicks using a CBR system. Expert Syst Appl 36(4):8239–8246
23. Narendra KS, Thathachar MAL (1974) Learning automata—a survey. IEEE Trans Syst Man Cybern SMC-4 4:323–334
24. n-Core (2011) n-Core: a faster and easier way to create wireless sensor networks. Retrieved 1 Sept from http://www.n-core.info
25. Nerguizian C, Despins C, Affès S (2004) Indoor geolocation with received signal strength fingerprinting technique and neural networks. Telecommunications and networking—ICT 2004. Springer Berlin/Heidelberg. pp 866–875
26. Nguyen H, Chan C (2004) Multiple neural networks for a long term time series forecast. Neural Comput Appl 13(1):90–98
27. Ray JK, Cannon ME, Fenton PC (1999) Mitigation of static carrier-phase multipath effects using multiple closely spaced antennas. Navig Wash 46(3):93–202
28. Rumelhart DE, Hinton GE, Williams RJ (1986) Learning representations by back-propagating errors. Nature 323(6088):533–536
29. Salcic Z, Chan E (2000) Mobile station positioning using GSM cellular phone and artificial neural networks. Wirel Pers Commun 14(3):235–254
30. Schmitz A, Wenig M (2006) The effect of the radio wave propagation model in mobile ad hoc networks. In: Proceedings of the 9th ACM international symposium on modeling analysis and simulation of wireless and mobile systems, Terromolinos, Spain, 2006, pp 61–67
31. Smola AJ, Schölkopf B (2004) A tutorial on support vector regression. Stat Comput 14(3):199–222
32. Stelios MA, Nick AD, Effie MT, Dimitris KM, Thomopoulos SCA (2008) An indoor localization platform for ambient assisted living using UWB. In: Proceedings of the 6th international conference on advances in mobile computing and multimedia, Linz, Austria, 2008, pp 178–182
33. Tapia DI, De Paz JF, Rodríguez S, Bajo J, Corchado JM (2008) Multi-agent system for security control on industrial Environments. Int Trans Syst Sci Appl J 4(3):222–226
34. Vapnik VN (1998) Statistical learning theory. Wiley-Interscience, New York
35. Xie JJ, Palmer R, Wild D (2005) Multipath mitigation technique in RF ranging. Electrical and Computer Engineering. Canadian Conference on 2005, pp 2139–2142
36. Yang Q, Li X, Shi X (2008) Cellular automata for simulating land use changes based on support vector machines. Comput Geosci 34(6):592–602
37. Yazdi HS, Rowhanimanesh A, Modares H (2011) A general insight into the effect of neuron structure on classification. Knowl Inf Syst. doi:10.1007/s10115-011-0392-6

Author Biographies

Juan F. De Paz Received a Ph.D. in Computer Science from the University of Salamanca (Spain) in 2010. He is Assistant Professor at the University of Salamanca and researcher at the BISITE research group (http://bisite.usal.es). He obtained a Technical Engineering in Systems Computer Sciences degree in 2003, an Engineering in Computer Sciences degree in 2005 at the University of Salamanca and Statistic degree in 2007 in the same University. He has been co-author of published papers in several journals, workshops and symposiums.

Dante I. Tapia Received a Ph.D. in Computer Science from the University of Salamanca (Spain) in 2009. At present, he is a researcher at the BISITE Research Group of the University of Salamanca (Spain). He obtained an Engineering in Computer Sciences degree in 2001 and an MSc in Telematics at the University of Colima (Mexico) in 2004. He has been involved in the development of automated systems in the Faculty of Telematics at the University of Colima and deeply collaborating with the Government of the State, where he obtained a scholarship to complete his academic formation. He has also been a coauthor of papers published in recognized workshops and symposiums.

Ricardo S. Alonso At present, he is a Ph.D. student at the University of Salamanca (Spain) under the supervision of Ph.D. Juan M. Corchado. He obtained an Engineering in Telecommunications degree in 2008 at the University of Valladolid (Spain) and an MSc in Intelligent Systems at the University of Salamanca (Spain) in 2009. He has also been a coauthor of papers published in recognized workshops and symposiums.

Cristian I. Pinzón Received a Ph.D. in Computer Science from the University of Salamanca (Spain) in 2010 and obtained a Master's degree in Intelligent Systems in the same university in 2007. He obtained a bachelor in Computer Sciences Degree at the Technological University of Panama in 2003 and a Technical Engineering in Systems Computer Sciences Degree at the same university in 2000. He has been co-author of published papers in several journals. His studies are supported by the Professional Excellence Program 2006-2010 IFARHU-SENACYT-Panama.

Javier Bajo Received a Ph.D. in Computer Science and Artificial Intelligence from the University of Salamanca in 2007. At present, he is Director of the Data Processing Center and Associate Professor at the Pontifical University of Salamanca (Spain) and researcher at the BISITE research group (http://bisite.usal.es) at the University of Salamanca (Spain). He obtained an Information Technology degree at the University of Valladolid (Spain) in 2001 and an Engineering in Computer Sciences degree at the Pontifical University of Salamanca in 2003. He has been a member of the organizing and scientific committee of several international symposiums such as CAEPIA, IDEAL, HAIS, etc. and is co-author of more than 170 papers published in recognized journals, workshops and symposiums.

Juan M. Corchado Received a Ph.D. in Computer Science from the University of Salamanca in 1998 and a Ph.D. in Artificial Intelligence (AI) from the University of Paisley, Glasgow (UK) in 2000. At present, he is Dean at the Faculty of Computer Sciences, Associate Professor, Director of the Intelligent Information System Group (http://bisite.usal.es) and Director of the MSc programs in Computer Science at the University of Salamanca (Spain). Previously, he was sub-director of the Computer Science School at the University of Vigo (Spain, 1999-00) and a Researcher at the University of Paisley (UK, 1995-98). He has been a research collaborator with the Plymouth Marine Laboratory (UK) since 1993. He has led several Artificial Intelligence research projects sponsored by Spanish and European public and private sector institutions and has supervised seven Ph.D. students. He is the co-author of over 230 books, book chapters, journal papers, technical reports, etc.